CAMD for entrainer screening of extractive distillation process based on new thermodynamic criteria

Stefano Cignitti[a], *Ivonne Rodriguez-Donis*[b,*], *Jens Abildskov*[a], *Xinqiang You*[c], *Nataliya Shcherbakova*[d], *Vincent Gerbaud*[d]

[a] *PROSYS, Department of Chemical and Biochemical Engineering, Technical University of Denmark, Building 229, 2800 Kgs Lyngby, Denmark*
[b] *Laboratoire de Chimie Agro-industrielle, LCA, Université de Toulouse, INRA, Toulouse, France*
[c] *State Key Laboratory of Chemical Engineering and Department of Chemistry, East China University of Science and Technology, Shanghai 200237, China*
[d] *Laboratoire de Génie Chimique, Université de Toulouse, CNRS, INP, UPS, Toulouse, France*

Keywords:
CAMD
Extractive distillation
Entrainer selection
Driving force
Isovolatility curves

A B S T R A C T

This paper presents a preliminary design framework for finding suitable homogeneous entrainers E to separate minimum boiling azeotropic mixtures AB by extractive distillation. The framework incorporates techniques such as Computer Aided Molecular Design (CAMD), addressing process needs and targeted thermodynamic properties. New thermodynamic criteria are considered for the entrainer design based on both, the thermodynamic properties of the binary mixtures AE and BE and the isovolatility curves in the ternary mixture ABE. In the CAMD problem, energy related property constraints on the boiling point and the vaporization enthalpy are also considered, leading to a mixed integer non-linear programming problem. Entrainer candidates are ranked by the maximization of the driving force of separation of A and B from their respective mixtures AE and BE under constraints limiting the entrainer composition for fixed values of the relative volatility. Further process optimization is done for validating the entrainer ranking by using Aspen plus V7.3, which minimizes the energy consumption and computes the total annual cost to compare different designs. The new thermodynamic criteria perform better than selectivity alone or a combined selectivity — capacity criterion, as proposed in the literature. The framework is illustrated through an entrainer problem design for the separation of acetone–methanol. Ethylene glycol is obtained as the best design solution. Comparison with conventional entrainers water and DMSO is carried out to validate the performance of the new criteria based on optimal process design study.

1. Introduction

The separation of azeotropic mixtures or close boiling components AB is a challenging task that requires non-conventional distillation processes, of which the azeotropic and extractive distillation processes are the most common (Arlt, 2014; Gerbaud and Rodriguez-Donis, 2014). Both processes involve the addition of an entrainer, E, that should interact differently with the mixture components A and B, causing their relative volatilities to either increase or decrease, and thereby enabling their separation. The selected entrainer and the thermody-

* *Corresponding author.*
E-mail address: ivonne.rodriguezdonis@ensiacet.fr (I. Rodriguez-Donis).
https://doi.org/10.1016/j.cherd.2019.04.038

namic topology of the ternary residue curve map (Kiva et al., 2003) mainly determine the efficacy of azeotropic and extractive distillation processes.

While there has been several works over the years devoted to entrainer selection for extractive distillation processes, there still exists a poor agreement between the preliminary ordering of the entrainers and the definite ranking confirmed by simulation/optimisation of the whole extractive distillation process. This is the task we challenge in this work. This paper is organized as follow. Section 2 surveys relevant literature about entrainer design criteria. Section 3 describes a novel framework based on Computer Aided Molecular Design that incorporates a novel thermodynamic criterion combining the driving force approach with isovolatility curve information and additional entrainer properties such as boiling point and vaporization enthalpy. Section 4 presents a case study that has been considered as benchmark in the literature: separation of acetone–methanol with entrainers by extractive distillation. The new framework is used to rank entrainers. Then the corresponding extractive distillation process is simulated and optimized, to evaluate the relevancy of the framework predictions.

2. State of the art

For the most common industrial process configurations, one can distinguish extractive from azeotropic distillation as the entrainer E is fed with the flow rate F_E at a different location than the of the mixture feeding F_{AB}, bringing an additional extractive section in the distillation column, between the rectifying and the stripping sections (Wahnschafft and Westerberg, 1993). Components A–B–E thermodynamic properties are well described using ternary residue curves diagrams, which can be arranged according to Serafimov's classification (Kiva et al., 2003). Fig. 1 highlights the column sections of the most typical flowsheet for the continuous and batch extractive distillation process enabling the separation of a minimum boiling azeotropic mixture using a heavy boiling homogeneous entrainer (1.0-1a Serafimov diagram class). Two connected distillation columns, the extractive distillation column and the entrainer recovery column, where the entrainer is always the bottom product of the second column and it is recycled to the extractive column, form the flowsheet in continuous operating mode (Fig.1a). Two column configurations are possible for the extractive column: direct (resp. indirect) split if the heavy entrainer binds to B (resp. A) and provides component A (resp. B) as distillate product (Fig. 1). In case of a batch process (Fig. 1b), the role of the stripping section is played by the composition changing into the reboiler. Furthermore, the extractive distillation with continuous entrainer feed step and the entrainer recovery step without entrainer feed, are performed sequentially in the same batch distillation column.

Design of the extractive distillation process is governed by the occurrence and location of the univolatility curve $\alpha_{A,B} = 1$ (Gerbaud et al., 2019). The univolatility curve is a particular type of isovolatility curve corresponding to the thermodynamic condition of the equality of the distribution coefficients $k_A = k_B$. The univolatility curve divides the composition triangle of residue curve maps into regions, distinguishable by the order of volatility of the components A and B. (Kiva et al., 2003). The topology of the residue curve map and the location of the univolatility curve $\alpha_{A,B}$ forms the core of a general feasibility criterion to infer which component A or B is the distillate product of the extractive column as well as the related column configuration for both, in continuous and batch operating mode (Rodríguez-Donis et al., 2009a; Shen et al., 2013). Laroche et al. (1991, 1992a,b) studied homogeneous extractive continuous distillation for separating minimum-boiling azeotropic mixtures with heavy, light and intermediate entrainers. Later, Rodríguez-Donis et al. (2009a,b, 2012a,b), Shen et al. (2013), Shen and Gerbaud (2013) and Shen et al. (2015) showed that the homogeneous extractive process with these entrainers is also feasible for the separation of maximum-boiling azeotropes and for binary mixtures with low relative volatilities by batch and continuous operating mode, respectively. These separations are represented by ternary diagrams which are readily described using Serafimov's classes (1.0-1a), (1.0-1b), (1.0-2), and (0.0-1) (Kiva et al., 2003). Noteworthy, (1.0-1a) class represents 21.6% of all azeotropic ternary diagrams (Kiva et al., 2003). It corresponds to the separation of a minimum boiling azeotropic mixture with a heavy boiling entrainer as it is the most abundant in industrial applications of extractive distillation processes. Kiva et al. survey (2003) pointed out that every azeotrope always belongs to an univolatility curve, but the opposite is not true. Hence, at least one univolatility curve exists in the Serafimov's ternary diagram class (1.0-1a) that is linked to the single binary azeotrope AB. Other possible univolatility curves as $\alpha_{A,E}$ and $\alpha_{B,E}$ have a poor effect in the feasibility of the extractive distillation process. Typical layout of the univolatility curves in the Serafimov's ternary diagram classes (1.0-1a), (1.0-1b), (1.0-2), and (0.0-1) involved in extractive distillation process are described in a series of papers of Rodríguez-Donis et al. (2009a,b, 2012a,b), Shen et al. (2013), Shen and Gerbaud (2013) and Shen et al. (2015).

The performance of the separation of a non-ideal mixture by extractive distillation relies on the choice of the entrainer (Lei et al., 2003). Gerbaud et al. (2019) published an extensive collection of extractive separation classes based on all Serafimov's classes suitable for extractive distillation, providing feasibility conditions, expected products and limiting conditions of operation parameters like entrainer flow rate and reflux ratio. For a given extractive separation class, the entrainer should possess features that are related to thermodynamics and to the process operation. We discuss the process operation first. According to the common practice, the best entrainer is deemed to carry out the separation with either lowest energy consumption or total annual cost (TAC) or both, although both criteria do not always imply the same optimum (You et al., 2015b). Energy consumption and TAC are primarily related to the minimum entrainer flow rate and the reflux ratio at the top of the extractive distillation column and the entrainer recovery column. Therefore, shortcut methods have been developed to determine the minimum values of these key operating parameters. The search of the limiting values of the reflux ratio and the entrainer flow rate for continuous operating mode can be done in a systematic fashion by the use of either an algebraic criterion (Levy et al., 1985; Petlyuk and Danilov, 1999; Petlyuk et al., 2015) or of mathematical approaches like bifurcation theory (Knapp and Doherty, 1994), or the combined bifurcation–rectification body method (Brüggemann and Marquardt, 2004). In particular, these methods enable to identify pinch branches. Firstly, the A-B-E ternary diagram must belong to feasible extractive distillation process classes, like the (1.0-1a) class which requires that a ternary saddle pinch point originating from a pure component (A or B) exists. In fact, the appearance of a ternary unstable node on the pinch branch originating at the azeotrope leads to an unfeasible separation (Knapp and Doherty, 1994). As the pinch branches depend on operating conditions, reflux ratio and entrainer flow rate, their knowledge give access to the minimum entrainer flow rate and the reflux ratio for the pro-

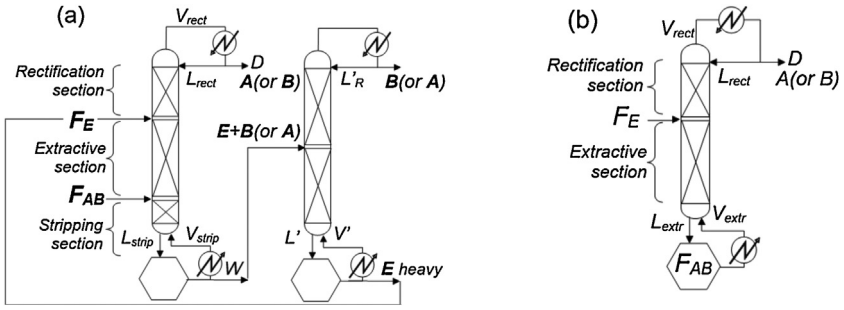

Fig. 1 – Typical flowsheets for the extractive distillation process. (a) Continuous direct split with a heavy entrainer (b) batch direct split with a heavy entrainer.

cess to be feasible, and hence, the related minimum energy demand for the extractive distillation process. For continuous extractive distillation, Kossack et al. (2008) used the Rectification Body Method (RBM) for computing pinch branches with a homotopic continuation method. The alternative infinite sharp split method requiring only VLE calculations has been recently proposed to compute these pinches (Petlyuk et al., 2015). For batch extractive distillation, Frits et al. (2006) used the interval arithmetic method for determining the limiting operating values for batch operating mode. Their study in batch operation agreed with that in continuous: the process is feasible under total reflux above a minimal entrainer flow rate, which corresponds to the merging of a stable pinch point at the edge AE (or BE) originating from the azeotrope with a saddle point originating from a pure component B (or A). They showed that decreasing the reflux ratio moved the pinch points inside the composition triangle and conveyed the extractive distillation boundaries generating infeasible regions. In general, feasible range of batch distillation processes is larger than the continuous one (Shen et al., 2013).

All the aforementioned shortcut methods require at first the selection of a suitable entrainer and this step involves the computation of thermodynamic features. For performing entrainer screening in extractive distillation processes, Pretel et al. (1994), Chen et al. (2005) and Kossack et al. (2008) proposed a systematic Computer Aided Molecular Design (CAMD) framework. The list of entrainer candidates was obtained from the computation of the selectivity $S^{\infty E}_{A,B}$ through the definition of the relative volatility at infinite entrainer dilution $\alpha^{\infty E}_{A,B}$, considering ideal gas behaviour and a constant ratio $\frac{P^0_A}{P^0_B}$:

$$\alpha^{\infty E}_{A,B} = \frac{\gamma^{\infty E}_A}{\gamma^{\infty E}_B} \cdot \frac{P^0_A}{P^0_B} \rightarrow S^{\infty E}_{A,B} = \frac{\gamma^{\infty E}_A}{\gamma^{\infty E}_B} \quad (1)$$

As Kossack et al. (2008) coupled the CAMD method with the flowsheet optimization using RBM models for generating a list of optimal entrainers and providing minimum energy demand and minimum entrainer flow rate $F_{E\min}$, they could verified the preliminary entrainer ranking with rigorous MINLP optimization of the whole process TAC (like in Fig. 1a). They concluded that $S^{\infty E}_{A,B}$ is a useful but not a very accurate criterion to screen entrainers. Setting a threshold of $S^{\infty E}_{A,B} > 2.4$ in the entrainers they compared, they observed that DMSO that binds to methanol, was ranked first in selectivity (UNIQUAC as thermodynamic model), first in low energy demand for the reboilers and second in TAC. They noted that due to the high boiling temperature of DMSO, steam at high pressure was required for the reboiler of each column. Furthermore, the whole process TAC correlated poorly with the selectivity criterion $S^{\infty E}_{A,B}$ for their case study, in contrast to Momoh (1991) who found for three case studies with many entrainers that selectivity correlated with the TAC (TAC computed without entrainer cost in this case). Both Momoh (1991) and Kossack et al. (2008) noted that entrainer selection based on selectivity $S^{\infty E}_{A,B}$ accentuates the weight of the cost of the extractive distillation column, compared to the cost of the entrainer recovery column, which is strongly dependent on the entrainer boiling point and vaporization enthalpy. Kossack et al. (2008) used this point to explain the DMSO ranking inversion when considering the extractive distillation column energy demand and the whole two column process sequence cost.

Hence, Kossack et al. (2008) proposed to rely upon a different criterion, namely the product $S^{\infty E}_{A,B}C^{\infty E}_B$ instead of constraining the two quantities individually:

$$S^{\infty E}_{A,B}C^{\infty E}_B = \frac{\gamma^{\infty E}_A}{\gamma^{\infty E}_B} \cdot \frac{1}{\gamma^{\infty E}_B} \quad (2)$$

The capacity $C^{\infty E}_B$ is a measure of the interaction between the component B and the entrainer E by showing a negative deviation from Raoult's law. It should be noted that selectivity and capacity of the entrainer increase with the decrease of the activity coefficient of component B at infinite dilution in E. Theoretically, entrainers with high selectivity $S^{\infty E}_{A,B}$ and capacity $C^{\infty E}_B$ may provide the separation of A and B with a low entrainer flow rate and reflux ratio, and therefore, with low energy consumption and total annual cost. Kossack et al. (2008) studied 14 entrainers to separate acetone–methanol mixture, ranking the entrainers on the basis of the selectivity $S^{\infty E}_{A,B}$ and the combination $S^{\infty E}_{A,B}C^{\infty E}_B$.

For comparing entrainers, let us define the relative difference percent in value X for the entrainer E compared to a reference entrainer:

$$RD^E_{ref}[Y] = \frac{Y_E - Y_{ref}}{Y_{ref}} \quad (3)$$

with Y being selectivity $S^{\infty E}_{A,B}$ or the combination $S^{\infty E}_{A,B}C^{\infty E}_B$ or the TAC.

DMSO was the best candidate of the entrainers that binds with methanol providing acetone as the distillate product in the extractive distillation column. Water ranked second, required 30% more TAC than DMSO. The smaller separation ability of water was measured via the relative difference in $S^{\infty E}_{A,B}$ and the combined criterion $S^{\infty E}_{A,B}C^{\infty E}_B$ resulting −17% and −80% respectively, with DMSO as reference entrainer. In the case of entrainers binding with acetone and enabling methanol as distillate, chlorobenzene beats *p*-xylene with a 22% smaller of TAC. Similarly, the relative difference in $S^{\infty E}_{A,B}$ and the combina-

Table 1 – Lower and upper bounds for the specified entrainer and process needs.

Product constraints				Process constraints			
Need	Lower	Upper	Constraint	Need	Lower	Upper	Constraint
n	2	6	Eq. (7)	K_E^{iE}	–	1	Eq. (11)
n_1	0	6	Eq. (8)	β_{AE} & β_{BE}	–	0	Eq. (12)
T_b(K)	–	473	Eq. (9)	β'_{AE} & β'_{BE}	0	–	Eq. (13)
ΔH_{vb}(kJ/mol)	–	65	Eq. (10)	$x_E^{(\alpha_{A,B}=1)}$	0	0.2	Eqs. (14) and (16)
				$x_E^{(\alpha_{A,B}=2)}$	0	0.7	Eqs. (15) and (16)

tion $S_{A,B}^{\infty E}C_B^{\infty E}$ were −60% and −81% respectively for *p*-xylene, with chlorobenzene as reference. These results show that there is a poor correlation between the relative difference of the process optimal cost RD_{ref}^{E} [TAC] (+%30% and +22%) and the relative difference of $S_{A,B}^{\infty E}C_B^{\infty E}$ (−80% vs −81%) for the second ranked entrainers water and *p*-xylene. Agreement with RD_{ref}^{E} [TAC] is even worst when considering the relative difference value of the selectivity criterion $RD_{ref}^{E}\left[S_{A,B}^{\infty E}\right]$ of −17% and −60% for water and *p*-xylene, respectively.

These works put in evidence that the entrainer capability for separating a mixture AB on a low cost basis cannot be evaluated in a reliable way based on thermodynamic parameters at infinite dilution with either Eqs. (1) or (2) criterion. Some reasons are the following. Firstly, information at infinite dilution provides limited information about the effect of the entrainer in the ternary composition space. That is required since the location of composition profiles in the rectifying and the stripping section in both distillation columns and the extractive section in the extractive distillation column span the whole ternary diagram. The actual effect of the entrainer on separating A and B is determined by the impact of the entrainer E over the full composition range of the binary vapor–liquid equilibrium AE and BE. Since Laroche et al. works, it has been established that the entrainer capability can be better judged from the iso- and univolatility curves. The univolatility curve has been used for preliminary design of the extractive distillation process in continuous and batch operating mode in order to determine the minimum entrainer flow rate and the feasible range of the reflux ratio (Lelkes et al., 1998; Shen et al., 2013; Shen and Gerbaud, 2013). Lelkes et al. (1998) proposed an equation for computing the minimum entrainer flowrate $F_{E\min}/V$ for batch extractive distillation at total reflux through a mass balance involving the distillate product and considering a pinch composition $\mathbf{x_P}$ at the entrainer feed stage. Indeed, this pinch composition at the entrainer feed tray matches the intersection of the univolatility curve $\alpha_{A,B}=1$ at the binary edge AE (or BE) for A (or B) as distillate product of the extractive distillation column. From a thermodynamic point of view, this intersection point $\mathbf{x_P}$ corresponds to the minimal amount of the entrainer $F_{E\min}$ for breaking the azeotropic mixture AB with feed F_{AB}. Later, Shen at al. (2013) proposed a relationship for computing the ratio $F_{E\min}/F_{AB}$ for a continuous extractive distillation column under a given reflux ratio R from the calculation of $F_{E\min}/V$ for a batch operating mode. The way $F_{E\min}/F_{AB}$ vary on the feasible interval of reflux ratio can be computed as suggested by Shen et al. (2013) and Shen and Gerbaud (2013). This simplified methodology allows reproducing reflux ratio or minimum energy demand versus entrainer-feed ratio feasible range diagrams in a similar way than earlier authors (Knapp and Doherty, 1994; Brüggemann and Marquardt, 2004). Despite the usefulness of feasible range diagram for engineers, the required knowledge of intersection point of the univolatility curve has been scarcely used for other purpose, like screening entrainer.

Another concept is the driving force concept (Gani and Bek-Pedersen, 2000) usefull to evaluate the effect of the entrainer on the binary vapour–liquid equilibrium of the mixtures AE and BE. It has been applied in numerous process synthesis (Babi et al., 2014; Tula et al., 2015) and design (Bek-Pedersen et al., 2000; Gani and Bek-Pedersen, 2000; Sánchez-Daza et al., 2003; Bek-Pedersen and Gani, 2004) works. For distillation process, the driving force is the difference between the equilibrium compositions of a target compound *i* in the vapour and the liquid phase of a binary mixture $i-j$ (see Eq. (4)). Driving force is a measure of the ease of a separation. This concept has not been used for the entrainer selection in extractive distillation so far. Below we refer to DF_i^{ij} as the maximal value over the composition range for binary $i-j$. Here, we combine the driving force approach with isovolatility curve information and additional entrainer properties such as boiling point and vaporization enthalpy in a CAMD problem formulation for designing a pure homogeneous entrainer for extractive distillation. The entrainer screening is based on the maximization of the driving force (DF) of the mixtures AE and BE and the composition of the entrainer x_E at the intersection point x_p of the isovolatility curves $\alpha_{A,B}$ on the side AE (resp. BE) for A (resp. B) as distillate product of the extractive distillation column, supplemented with boiling point and vaporization enthalpy constraints. The framework of Cignitti et al. (2015) is then used to convert the CAMD problem into a mixed integer non-linear programming problem (MINLP). For illustration, the entrainer design problem for the separation of the azeotropic binary mixture acetone–methanol by extractive distillation is chosen. The best entrainer from the CAMD search is compared with conventional entrainers, using Aspen plus V7.3 to minimize the energy consumption where the total annual cost is also calculated to compare the different designs.

3. CAMD framework for design of homogeneous entrainer for extractive distillation process

The proposed computer-aided framework for the design of pure homogeneous entrainers for extractive distillation processes utilizes a thermodynamic criterion that includes process needs and target physico-chemical properties to enunciate a CAMD problem that is transformed into an MINLP formulation. The MINLP formulation is then solved through a decomposed approach. The thermodynamic criterion combines the driving force approach with isovolatility curve information and additional entrainer properties such as boiling point and vaporization enthalpy.

The CAMD framework has four steps detailed here as adopted by Cignitti et al. (2015):

3.1. Step 1: problem definition

The process needs and target properties of the entrainers are first defined. These can be thermodynamic properties, economic, and environmental needs. The product type refers to the desired molecule and its type (acyclic, cyclic, aromatic etc.) and to the type and the occurrence of limitations on the functional groups. Following the insight of process feasibility related to extractive distillation, BE (or AE) is separated in the entrainer recovery column, depending on whether the A (or B) is the distillate product in the extractive distillation column. For simplification, each alternative is solved separately. The entrainer is also constrained to be fully miscible with A and B and to not form additional azeotropes. To avoid heavy process energy requirements, the use of an entrainer with a low boiling point and vaporization enthalpy is enforced.

3.2. Step 2: CAMD formulation

The CAMD model uses a set of constraints that describe chemically feasible molecules in combination with GC property prediction functions. Among 220 first order groups available from Hukkerikar et al. (2012), only acyclic solvents containing C, H and/or O atoms are considered for the sake of simplicity. Thus, the group set G_1 only contains linear acyclic groups containing C, H and/or atoms (G_1 = {CH_3, CH_2, CH, C, OH, CHO, CH_3COO, CH_2COO, HCOO, CH_3CO, CH_2O, HCO, COOH, COO}). Water, methanol (CH_3OH) and ethylene glycol ($C_2H_6O_2$) are separate groups in UNIFAC, so we evaluate them as candidates separately. Through classification of the different structural groups based on their valencies, the octet rule (Eq. (5)) provides a simple relation for the structural feasibility of a given collection of groups (Odele and Macchietto, 1993). Eq. (6) states the single bonds between groups. The parameter n_i is the number of first-order groups G_1 of set i in the target molecule and v_i the valency of group i. Eq. (7) ensures the lower and upper bounds on the number n_1 while Eq. (8) constrains the total number of groups n making up the whole molecular structure of a given molecule. Table 1 displays their respective lower and upper values.

The process need regarding an energy efficient entrainer is expressed via a low boiling temperature (T_b) (Eq. (9)) and low vaporization enthalpy (ΔH_{vb}) (Eq. (10)). The thermodynamic process need of non-formation of binary azeotrope with A and/or B is verified through the computation of the distribution coefficient of E in the respective binary mixtures AE and BE according to the constraint Eq. (11). Complete miscibility of the entrainer with the components A and B is ensured by constraining the value Eq. (12) and the respective second derivatives Eq. (13) of Gibbs free energy of mixing (β and β') of the mixtures AE and BE, respectively, to limit values displayed in Table 1 (Conte et al., 2011).

As the objective function, the driving force (DF) of the binary mixture AE and BE should be maximized at the same time while the entrainer composition x_E of the intersection of the isovolatility values $\alpha_{A,B} = 1$ and $\alpha_{A,B} = 2$ at the binary edge AE (or BE) are considered as constraints (Eqs. (14)–(16)). Solutions of Eqs. (14)–(16) also indicate which component A or B is withdrawn as distillate product in the extractive distillation column.

3.3. Step 3: MINLP formulation

The general CAMD problem is converted into an MINLP problem with structural feasibility constraints, pure component property constraints and process constraints. **N** is an array of integer variables, related to the numbers of the building blocks and/or molecules (1st order groups). **Y** is an adjacency matrix which is related to the description of the molecular structure. **X** is a vector of continuous variables, related to the phase equilibrium models of binary and ternary mixtures. Commonly, one is interested in optimizing a process variable or metric, such as a performance measure, subject to product and process constraints. The target for the process is to maximize the driving force of the mixture AE and BE. Eq. (4) represents the mathematical formulation of the objective function.

Based on CAMD formulation, the MINLP problem is written as:

$$\text{Max } F_{obj} = \left|DF_A^{AE}\right| + \left|DF_B^{BE}\right| = \left|y_A - x_A\right|_{AE} + \left|y_B - x_B\right|_{BE} \tag{4}$$

Subject to:
structural contraints: $g_1(\mathbf{N}, \mathbf{Y}) \leq 0$

$$\sum_{i_1=G_1} \left(2 - v_{i_1}\right) n_{i_1} = 2 \tag{5}$$

$$\sum_{i_1 \neq i_2;} n_{i_2} > \left(v_{i_1} - 2\right) + 2 \forall i_1, i_2 \in G_1 \tag{6}$$

$$n_{i_1}^L \leq n_{i_1} \leq n_{i_1}^U \tag{7}$$

$$n^L \leq \sum_{i_1 \in G_1} n_{i_1} \leq n^U \tag{8}$$

pure component property constraints: $g_2(\mathbf{N}) \leq 0$

$$T_B \leq 204.359.log \sum_m N_m T_{bm} \tag{9}$$

$$\Delta H_{vb} \leq \Delta H_{vb0} + \sum_m N_m \Delta H_{vbm} \tag{10}$$

thermodynamic model constraints: $g_3(\mathbf{X}, \mathbf{N}) \leq 0$

$$\frac{\gamma_E{}^* P_E^0}{P_T} < K_E^{iE} \tag{11}$$

$$\sum_l x_l.ln\gamma_l + \sum_l x_l.lnx_l \leq \beta_{iE} \tag{12}$$

$$\frac{\partial^2 \left(\sum_l x_l{}^* ln\gamma_l + \sum_l x_l{}^* lnx_l\right)}{\partial x_i^2} \geq \beta'_{iE} \tag{13}$$

$$\left(P_A^O.\gamma_A^{AE}\right) / \left(P_B^O.\gamma_B^{\infty AE}\right) - 1 = 0 \tag{14}$$

$$\left(P_A^O.\gamma_A^{AE}\right) / \left(P_B^O.\gamma_B^{\infty AE}\right) - 2 = 0 \tag{15}$$

$$(1 - x_E).P_A^{O*}\gamma_A^{AE} + x_E.P_E^{O*}\gamma_E^{AE} - P_T = 0 \tag{16}$$

Here i $\in$ {A,B}, γ_l is the activity coefficient of component $l \in$ {A,B,E}. P^O is the vapour pressure computed from Antoine parameters reproducing the normal boiling point, critical point and acentric factor of the pure component in question. Finally, P_T = 1 atm.

3.4. *Step 4: solution of MINLP problem*

The solution of the MINLP is obtained with GAMS (BIBLIO). LINDOGlobal is selected as the MINLP solver for the simultaneous solution strategy (Bussieck and Meeraus, 2004). A database is used for group contribution coefficients for the molecular groups. Group contributions for predicting pure compound properties used in this work are those of Constantinou and Gani (1994) and Constantinou et al. (1995). Computation of the phase equilibrium for binary and ternary mixture was carried out using UNIFAC (Fredenslund et al., 1975 and subsequent parameters). Therefore, the solution of the CAMD problem involves nonlinear property models. The decomposed optimization approach to solve a large MINLP formulation including an integrated chemical product and process design framework was proposed by Cignitti et al. (2015). The computer-aided design framework was successfully applied for the molecular design of solvents (pure component or mixture) for a solvent extraction case study involving the separation of acetic acid and water.

4. Case study: separation of acetone–methanol using a heavy entrainer

4.1. *MINLP solution of the CAMD framework for optimal entrainer design*

In this work we consider the extractive distillation of the minimum boiling azeotrope acetone (A)–methanol (B) with a heavy entrainer (E), belonging to the most studied and frequent extractive separation diagram class (1.0-1a). The acetone–methanol mixture is the main component in the aqueous product obtained from hydrocarbon syntheses by the Fischer–Tropsch process. Depending on the entrainer, either acetone or methanol can be recovered as product, giving rise to two subsets of extractive separation classes described in Gerbaud et al. (2019). Acetone (A) is recovered when the entrainer (E) preferentially interact with methanol and the univolatility curve $\alpha_{A,B} = 1$ goes towards the AE edge (extractive separation class (1.0-1a)-m1). We focus on this class in this paper. When $\alpha_{A,B} = 1$ goes towards the BE edge, methanol is the distillate product of the extractive column (extractive separation class (1.0-1a)-m2).

We apply the CAMD framework for the most studied flowsheet structure giving acetone as distillate product of the extractive column. Most papers devoted to this flowsheet structure involves water and DMSO as heavy entrainers. Luyben and Chien (2010) studied the influence of the entrainer on the dynamic controllability of the two distillation columns in the extractive sequence and opted for DMSO as the optimal entrainer. Skiborowski et al. (2015) used Kossack and coworkers's list (Kossack et al., 2008) and also found DMSO as the most suitable entrainer by using an evolutionary algorithm for optimizing the design of the extractive distillation process. Alternatively, an optimal flowsheet with water as entrainer was later designed and improved by You et al. (2014), by proposing a new objective function for the minimization of the total energy consumption related to the total distillate flow rate. You et al., 2015a, 2016) also pointed out the advantage of decreasing the working pressure of the extractive distillation column due to a more favourable location of the isovolatility curve $\alpha_{A,B} = 1$ closer to the acetone apex. This location hinted that under vacuum condition, separation of the azeotropic components requires lower entrainer flow rate and reflux ratio. In the present work, water and DMSO are both considered as the benchmark entrainers for the separation of acetone–methanol by extractive distillation process.

The MINLP problem cannot be solved directly due to its size. The main contributing factor here is the computer intensive calculations of UNIFAC equations and the many conditions requiring individual step-wise constraints (e.g. azeotrope, miscibility and isovolatility). Thus, the decomposed solution strategy is used and the solution approach selection workflow is detailed in Cignitti et al. (2015). First, the initial list of molecular structure candidates is generated by solving the constraints (5)–(10) (molecular structure and pure properties combined). NLP problems are then solved along with the objective function from Eq. (4) with constraints to (11)–(16).

As a result of the application of the CAMD framework, ethylene glycol (EG) is found as the optimal entrainer, which provides the maximum value of the driving force for the binary mixtures AE and BE along with the lower composition of the entrainer satisfying the constraints Eqs. (14)–(16). EG was earlier proposed by Kossack et al. (2008) who also noted that it is more environmentally benign than DMSO on the basis of the CAMD problem they solved. However, it was further rejected because no solution was found with the RBM approach they processed afterwards.

Table 2 displays the physical properties and the thermodynamic parameters defined in Table 1 of the benchmark entrainers (water and DMSO) as well as those computed for EG. Computation of the thermodynamic parameters for water and DMSO was carried out using UNIQUAC model with binary coefficients available Aspen plus V7.3 while UNIFAC method (Fredenslund et al., 1975) was used for EG. The maximum value of the driving force (DF_A^{AE}; DF_B^{BE}) for the respective binary mixtures AE and BE and the entrainer composition for a given relative volatility is also reported in Table 2. EG does not form any azeotrope with A and B, and their respective mixtures AE and BE are homogeneous. EG provides a driving force of the component A and B in their respective mixture AE and BE that is higher than DMSO, so far claimed to be the best entrainer in the literature for the extractive distillation of acetone–methanol (Table 2). Compositions of the entrainer at the isovolatility line intersection with the AE edge $x_E^{(\alpha_{A,B}=1)}$ and $x_E^{(\alpha_{A,B}=2)}$ are slightly greater than those computed for DMSO. According to the extractive distillation feasibility insight, this means that EG is able to separate acetone and methanol with a low entrainer flow rate and reflux ratio in both distillation columns. Therefore, it hints at a process possibly with lower energy consumption and TAC.

First we evaluate the new entrainer EG with respect to the criteria used in the literature, $S_{A,B}^{\infty E}$ and $S_{A,B}^{\infty E}C_B^{\infty E}$. Fig. 2 displays isovolatility curves diagrams for the ternary mixture of acetone–methanol–entrainer for water, DMSO and EG at atmospheric pressure (1 atm). The values of selectivity at infinite dilution $S_{A,B}^{\infty E}$ are 2.41, 2.88 and 2.99 for water, DMSO and EG, respectively. According to this criterion, the three entrainers have similar ability to separate the acetone–methanol azeotrope. It can be seen in Fig. 2 that DMSO and EG show a similar portrait of the isovolatility curves reaching a maximum value at an intermediate composition of the entrainer on the edge methanol–entrainer. Conversely, the isovolatility increases monotonically with the entrainer composition for water and reaches the maximum value at the edge acetone–water close to the water apex. Regarding the isovolatility curves of $\alpha_{A,B} = 1$ and $\alpha_{A,B} = 2$, the entrainer com-

Table 2 – Comparison of the optimal design entrainer by CAMD (EG) with benchmark entrainers (Water and DMSO).

Entrainers	T_b(K)	ΔH_{vb}(kJ/mol)	K_E^{AE}	K_E^{BE}	β_{AE} β_{AE}	β'_{AE} β'_{BE}	DF_A^{AE}	DF_B^{BE}	$x_E^{(\alpha_{A,B}=1)}$	$x_E^{(\alpha_{A,B}=2)}$	$S_{A,B}^{\infty E}$	$S_{A,B}^{\infty E}C_B^{\infty E}$
Water	273	40.8	<1	<1	<0	>0	0.6308	0.3843	0.172	0.600	2.41	1.10
DMSO	462	43.8	<1	<1	<0	>0	0.8016	0.6883	0.115	0.471	2.88	5.57
EG	470	64.5	<1	<1	<0	>0	0.9104	0.8284	0.129	0.511	2.99	2.39

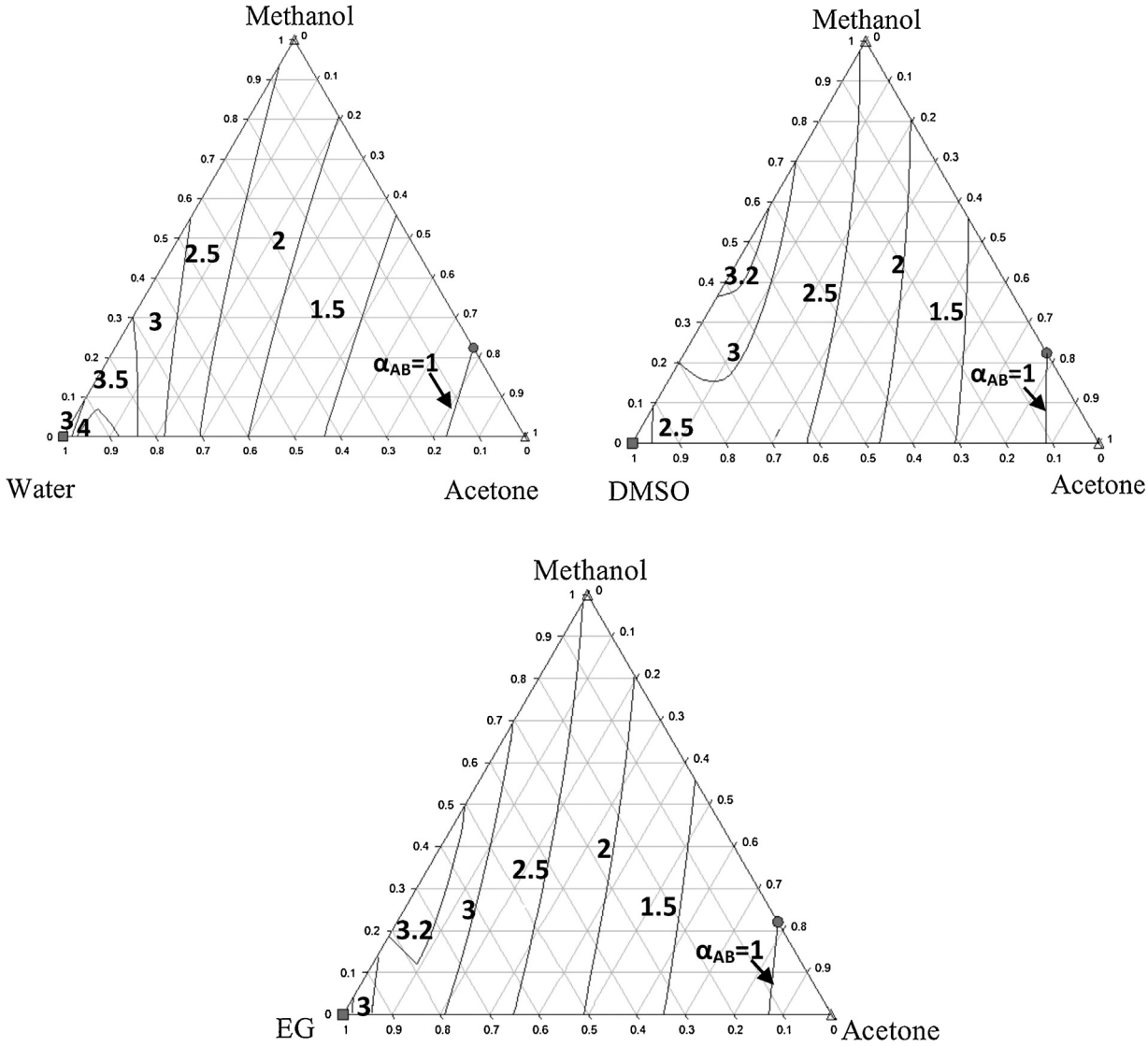

Fig. 2 – Isovolatility curves chart for the ternary mixture acetone–methanol–entrainer.

positions x_E are comparable (see Table 2) for DMSO and EG with a slight edge for DMSO. Therefore, separation using ethylene glycol may require a slightly higher minimum entrainer flow rate.

The combined criterion $S_{A,B}^{\infty E}C_B^{\infty E}$ values are 1.1, 5.57 and 2.39 for water, DMSO and EG, respectively. Water seems to be a very poor entrainer because the value is near unity. However, water has been widely used for the separation of this azeotropic mixture industrially. This combined criterion is therefore not discriminant on the basis of the industrial practice. Furthermore, one can expect a significant difference between the optimal flowsheet for DMSO and ethylene glycol. Process optimization results will be presented in the next Section 4.2.

Second, we evaluate EG with respect to the new criterion that was used in the CAMD search, combining and analysis of the topology of the isovolatility curve maps and the driving force measure. Fig. 3 displays the driving forces of the binary mixtures AE and BE for the three entrainers from the vapour–liquid equilibrium at P = 1 atm. One can observe that there is a significant difference between the maximum value of the driving force for the components A and B for water and DMSO. EG, the optimal solution of the CAMD problem, increases by 0.1 the driving force of A and B compared to DMSO and by 0.3 compared to water.

4.2. *Optimization studies for comparison of benchmark entrainers and ethylene glycol*

In this section we evaluate the CAMD-based superiority of ethylene glycol over benchmark entrainers water and DMSO, by simulating and optimizing the extractive distillation process described in Fig. 1a. In the case of DMSO, Kossack et al. (2008) and Skiborowski et al. (2015) did the optimization with the successive relaxation and hybrid

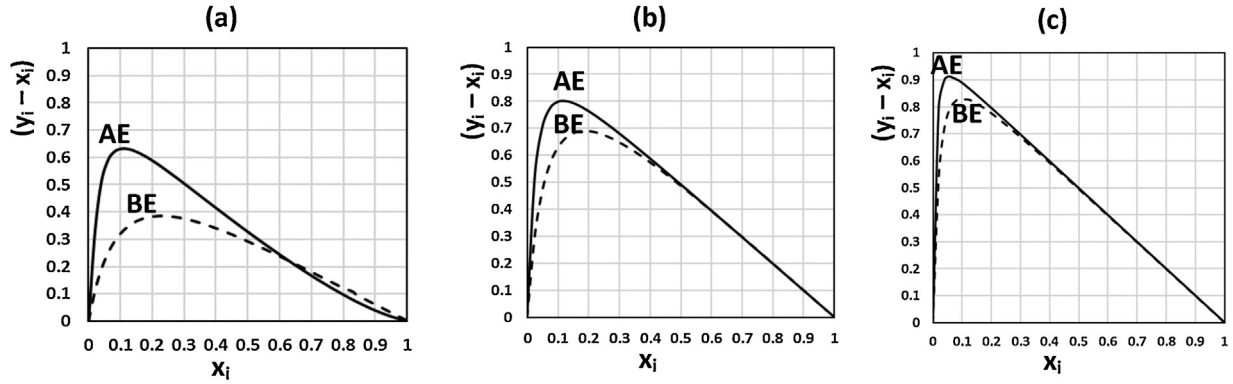

Fig. 3 – Driving force of mixtures AE and BE for E = water (a), E = DMSO (b) and E = EG (c). i = A or B.

evolutionary-deterministic MINLP solving techniques respectively. In this work, we use a classical simpler sequential technique (De Figueirêdo et al., 2011). It was also carried out to optimize the extractive distillation process for separating acetone–methanol with water as entrainer (Luyben and Chien, 2010; You et al., 2014, 2015a,b).

While other works minimized TAC, here we minimize the process energy consumption according to the equation proposed in our previous work (You et al., 2014, 2015a,b) dealing with the optimization of the extractive distillation separation of acetone–methanol using water. TAC is computed afterwards.

$$\text{MINOF} = \frac{M.Q_{r1} + m.Q_{c1} + M.Q_{r2} + m.Q_{c2}}{D_A + D_B} \tag{17}$$

$$\text{Subject to}: x_{acetone,\,D_A} \geq 0.995 \tag{17.1}$$

$$x_{acetone,\,W_1} \leq 0.001 \tag{17.2}$$

$$x_{methanol,\,D_B} \geq 0.995 \tag{17.3}$$

$$x_{entrainer,\,W_2} \geq 0.9999 \tag{17.4}$$

The meaning of OF is the total energy consumption used per total product unit flow rate (kJ/kmol). Constraint Eq. (17.1) concerns the acetone purity in the distillate while constraint Eq. (17.2) in bottom W_1 aims at keeping high the product acetone recovery of the extractive distillation column. Constraint Eq. (17.3) deals with the methanol purity in distillate of the entrainer recovery column and constraint Eq. (17.4) focuses on the recycling entrainer purity. The meanings of the notations Q_{r1}, Q_{c1}, Q_{r2}, Q_{c2}, D_A and D_B are the reboiler and condenser heat duties, distillate flow rates of extractive column and the entrainer recovery column, respectively, as shown in Fig. 1. The energy price difference factor m equals to 0.036 for condenser (cooling water). M may equal to 1, 1.065 or 1.280 when low, middle or high pressure steams are used, respectively (You et al., 2014, 2015a,b, 2016).

The MINLP problem is solved by Aspen plus V7.3 simulator built-in SQP method using a two-step optimization methodology (de Figueirêdo et al., 2011; You et al., 2014). First for a given number of trays of the columns N_1 (extractive column) and N_2 (entrainer recovery column) and considering an open loop flowsheet with no entrainer recycle, the sequential quadratic programming (SQP) method is used for process optimization under product purity and recovery constraints to ease the convergence of the process. The control variables are reflux ratios R_1, R_2 of each columns of the flowsheet (see Fig. 1) and the entrainer flow rate F_E. Secondly, a sensitivity analysis is performed to find the optimal values of two distillate flow rates D_A and D_B (see Fig. 1) and the three feed tray locations NF_E, NF_{AB}, N_{E+B}, while SQP is run for each set of discrete variable values. The final optimisation is done by minimizing energy consumption and it is validated by re-running the simulation in a closed-loop flowsheet. Finally, the TAC is calculated to compare the different designs.

TAC has been commonly used as an optimization criterion (Kossack et al., 2008). Here it will be evaluated from the optimal operating values of the solution of OF. TAC includes capital cost per year and operating costs:

$$TAC = \frac{capital\,cost}{payback\,period} + operating\,costs \tag{18}$$

For computing the capital cost, the Douglas, 1988 are employed after correcting the CEPCI inflation index. The column shell, tray and heat exchanger cost constitute the capital cost and their formulae are shown in appendix A. The CEPCI of 2013 (567.3) and a three-year payback period are used for calculating the capital cost (CEPCI, 2016). The operating cost includes the energy cost in reboiler and condenser. The heat exchanger for cooling the recycling entrainer is taken into account in order to emphasize its effect on the process. Other costs such as the liquid delivery pumps, pipes, valves were neglected at the conceptual design stage that we consider.

Table 3 displays the optimization results. DMSO provides the separation of acetone–methanol with the lowest energy consumption and the lowest total annual cost (TAC), beating EG by a few percent (2.8%), which was the best choice from the optimal solution of the CAMD framework. One drawback of using EG lies on its boiling temperature and vaporization enthalpy higher than DMSO, which results in a greater heat duty $Q_{reboiler}$ in the entrainer recovery column. The optimal design values are comparable for the benchmark entrainers with those found in the literature. According to the supplementary material file of the extractive distillation review, listing extractive distillation processes published in the literature (Gerbaud et al., 2019), the process with EG has been studied only by a few authors and has not been optimized before. For water, Luyben's design with 57 total trays in the extractive column and 15 trays in the extractive section required more entrainer (1100 kmol/h) (Luyben and Chien, 2010). You and coworkers showed that the increase of the total number of trays and also of the tray number in the extractive section was beneficial for the TAC and OF (You et al., 2015a). For DMSO, results are also comparable to the published literature with 35 trays and 536 kmol/h of entrainer (Kossack et al.,

Table 3 – Optimized values of the operating conditions for water, DMSO and ethylene glycol.

Entrainers	Water		DMSO		Ethylene glycol	
Parameters	Extractive column	Recovery column	Extractive column	Recovery column	Extractive column	Recovery column
Total trays	82	26	41	13	58	7
Rectifying trays	37	16	2	4	2	3
Extractive trays	28	–	24	–	26	–
Stripping trays	15	8	13	7	28	2
F_{AB} (kmol/h)	540.0	–	540.0	–	540.0	–
F_E (kmol/h)	844.8	–	402.8	–	445.6	–
Reflux ratio	2.46	1.3	1.408	0.09	1.448	0.05
D (kmol/h)	271	271.1	270.5	270.5	270.3	270.2
$Q_{condenser}$ (MW)	7.702	6.095	5.361	2.937	5.442	2.815
$Q_{Reboiler}$ (MW)	8.825	6.195	6.88	4.318	6.901	4.75
TAC (10^6\$)	4.348 (+31.4%)		3.309 (0%)		3.398 (+2.8%)	
OF (MJ/kmol)	29.8169 (+34.5%)		22.1641 (0%)		23.0547 (+4.0%)	

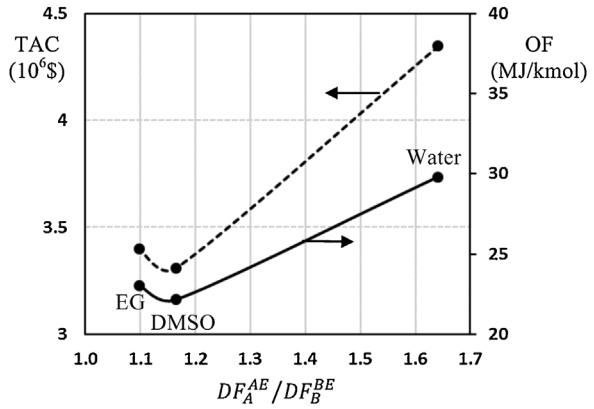

Fig. 4 – MINLP results of energy consumption (OF) and TAC as a function of the ratio of driving forces of A and B in their respective mixtures AE and BE.

2008). Kossack et al. (2008) also evaluated a +30.5% extra cost for water compared to DMSO, similar to +31.4% found in this study.

A major argument in favour of using our new criteria based on driving force and isovolatility comes from EG results. Indeed although optimized process results show that it allows the separation at cost and energy comparable to DMSO (Table 3), EG is not so favorable according to the literature criteria, namely selectivity ($S_{A,B}^{\infty E} = 2.99$) and combined selectivity–capacity ($S_{A,B}^{\infty E} C_B^{\infty E} = 2.39$) compared to the best benchmark entrainer DMSO ($S_{A,B}^{\infty E} = 2.88$ and $S_{A,B}^{\infty E} C_B^{\infty E} = 5.57$). In particular, the selectivity–capacity difference is remarkably large. On the other hand, the isovolatility values and the driving forces are similar for DMSO and EG (Table 2). Fig. 4 shows that both OF and the TAC follow the same trend as the driving force ratio DF_A^{AE}/DF_B^{BE}. It seems that an optimal separation of A and B in the extractive distillation column is related to an optimal difference ratio between the maximum value of the driving force of A and B in their respective AE and BE mixtures. Although one could define a criterion based on the ratio between the driving forces of A in AE to B in BE, the definitive set of an optimal difference ratio between them requires more extensive optimization studies including a large variety of case studies.

Regarding isovolatility curves, Fig. 5 shows also that $x_E^{(\alpha_{A,B}=1)}$ and $x_E^{(\alpha_{A,B}=2)}$ evolution trends follow those of OF and TAC. Despite limited number of points, we display in Fig. 5 linear regressions with coefficients R^2 are higher than 0.94. Kossac et al. (2008) found that the capability of the screening heuristic $S_{A,B}^{\infty E} C_B^{\infty E}$ to predict the process cost was twice better (linear regression constant R2 = 0.8749) than the selectivity criterion alone $S_{A,B}^{\infty E}$ by considering five coupling of entrainer candidate and thermodynamic model (UNIQUAC: DMSO, water, chlorobenzene and *p*-xylene; UNIFAC original: *p*-xylene).

Fig. 6 displays parity plot to compare all four criteria: selectivity $S_{A,B}^{\infty E}$, selectivity capacity $S_{A,B}^{\infty E} C_B^{\infty E}$, driving force ratio DF_A^{AE}/DF_B^{BE} and isovolatility curves $x_E^{(\alpha_{A,B}=1)} + x_E^{(\alpha_{A,B}=2)}$ with the relative deviation of TAC and OF. Relative deviations (%) of parameters were computed by Eq. (3) taking DMSO as the reference optimal entrainer. It can be observed in Fig. 6 that the new selectivity criteria, DF_A^{AE}/DF_B^{BE} and $x_E^{(\alpha_{A,B}=1)} + x_E^{(\alpha_{A,B}=2)}$, that we have used in the CAMD problem are the closest to the bisector. They are more prone to hint at the extractive distillation process cost (TAC) and energy consumption (OF) than the first two so far widely used in the literature. These results show the better reliability of the new thermodynamic based criteria, DF_A^{AE}/DF_B^{BE} and x_E for $\alpha_{A,B} = 1$ and $\alpha_{A,B} = 2$ to screen entrainers allowing the separation of binary azeotropic mixtures belonging to Serafimov's class (1.0-1a)-m1 by direct split extractive column configuration. The methodology can be extended to screen entrainers in (1.0-1a)-m2 class that bind with acetone, as well as to other feasible Serafimov's ternary diagram classes (1.0-1b), (1.0-2) and (0.0-1) for extractive distillation process.

4.3. *Analysis of the design of optimal extractive distillation process of benchmark entrainers and ethylene glycol*

In this section, we explore process and thermodynamic insights to understand why the new driving force and isovolatility based criteria match better with cost and energy consumption than selectivity and combined selectivity–capacity criteria commonly used in literature.

Our proposal of considering the driving force becomes relevant when discussing the entrainer flow rate values for each optimal process design. Process feasibility argues that the univolatility curve $\alpha_{A,B} = 1$ intersection with the binary edge AE is correlated with the minimum entrainer flow rate. Indeed there is a correspondence between the ranking of the $x_E^{(\alpha_{A,B}=1)}$ value (Table 2) and the optimal entrainer flow rate ranking (Table 3). However, one could not expect a doubling of the water optimal flow rate on the sole basis of the univolatility curve intersection differences. On the other hand, if we add to the minimum entrainer flow rate information the knowledge of the driving force maps DF_A^{AE} and DF_B^{BE} (Fig. 3), we can explain our results readily. Similar $x_E^{(\alpha_{A,B}=1)}$ and $x_E^{(\alpha_{A,B}=2)}$ values

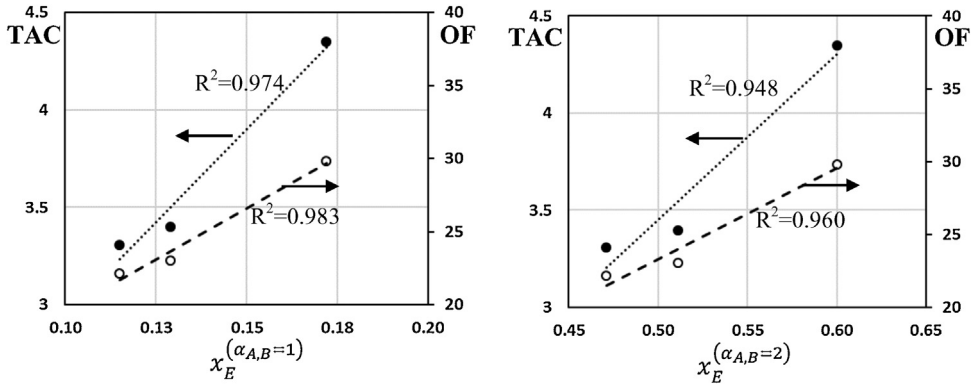

Fig. 5 – MINLP results of energy consumption (OF) and TAC as a function of the entrainer composition on the side AE for isovolatility curves $\alpha_{A,B} = 1$ and $\alpha_{A,B} = 2$.

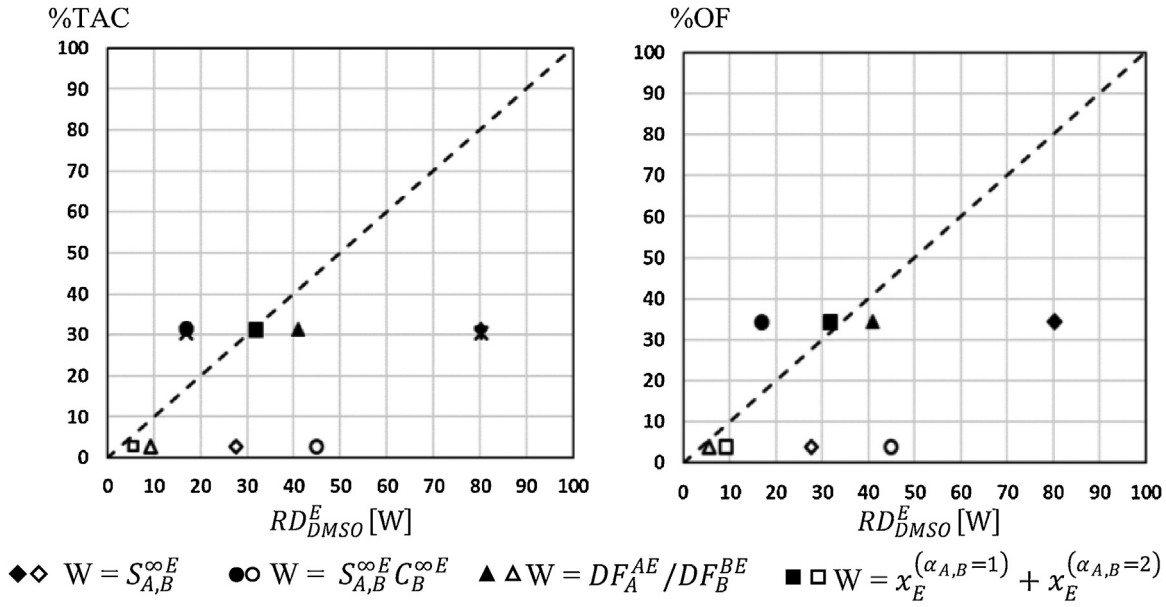

Fig. 6 – Deviation percentage as a function of relative deviation RD^E_{DMSO} [W] defined in Eq. (3) for four criteria compared to DMSO. Filled symbols: E = water. Empty symbols: E = EG.

and driving force DF^{AE}_{A} >0.8 (see Table 2) give rise to comparable and low entrainer flow rate and reflux ratio for DMSO and ethylene glycol in the extractive distillation column. Higher entrainer composition related to isovolatility curves location and lower driving force values for water resulted in a higher entrainer flow rate and a larger reflux ratio.

It is also important to consider how driving forces influence the design of each column. According to Tables 2 and 3, lower driving forces hint at more difficult and costly separation: more trays, and more heat duty (correlated with a much higher entrainer flow rate and reflux ratio). In the case of EG, the higher driving forces DF^{AE}_{A} and DF^{BE}_{B} facilitate the separation of acetone (A) in the rectifying section of the extractive column and of methanol (B) in the entrainer recovery column. Nevertheless, a competitive phenomenon between A and B must occur inside the extractive and the stripping section of the extractive distillation column due to the closeness of forces DF^{AE}_{A} and DF^{BE}_{B} curves (Fig. 3c). Besides, the necessary low composition of acetone in the bottom stream (translated as constraint 2 in the CAMD problem) requires twice the number of equilibrium trays in the stripping section compared to DMSO.

Fig. 7 displays the optimal liquid profile in the extractive column and the entrainer recovery distillation column along with the driving force curves of AE and BE. We focus on the extractive section for two reasons: This is where the main feed is depleted from the unwanted compound (B in our case) and the composition location at the entrainer feed tray (so-called stable node of the extractive section) governs the process feasibility (Rodríguez-Donis et al., 2009a; Shen et al., 2013; Gerbaud et al., 2019). Fig. 7 shows that the liquid profile in the extractive section — between the two feeds F_E and F_{AB} — lies in a region where the driving force of acetone DF^{AE}_{A} are similar for ethylene glycol and DMSO (Fig. 7b and c) and it is lower for water (Fig. 7a). However, the number of equilibrium trays in the extractive section are similar for the water, DMSO and EG (28, 24 and 26 respectively). The fact that the reflux ratio is similar for DMSO and EG while being the double for water needs another explanation. Composition profiles in the extractive sections depend on reflux ratio and entrainer flow rate (Gerbaud et al., 2019). Due to the lower driving force extrema, water needs nearly double entrainer flow rate and reflux ratio than DMSO or EG to break the azeotrope acetone–methanol with similar number of trays in the extractive section. Combined with a higher entrainer flow rate, heat duty in the extractive column is greater for water and process cost rises.

Regarding the entrainer recovery column, the optimal feed location for ethylene glycol corresponds to the highest driving force of the three entrainers (DF^{BE}_{B} = 0.62 in Fig. 7f). Hence, ethy-

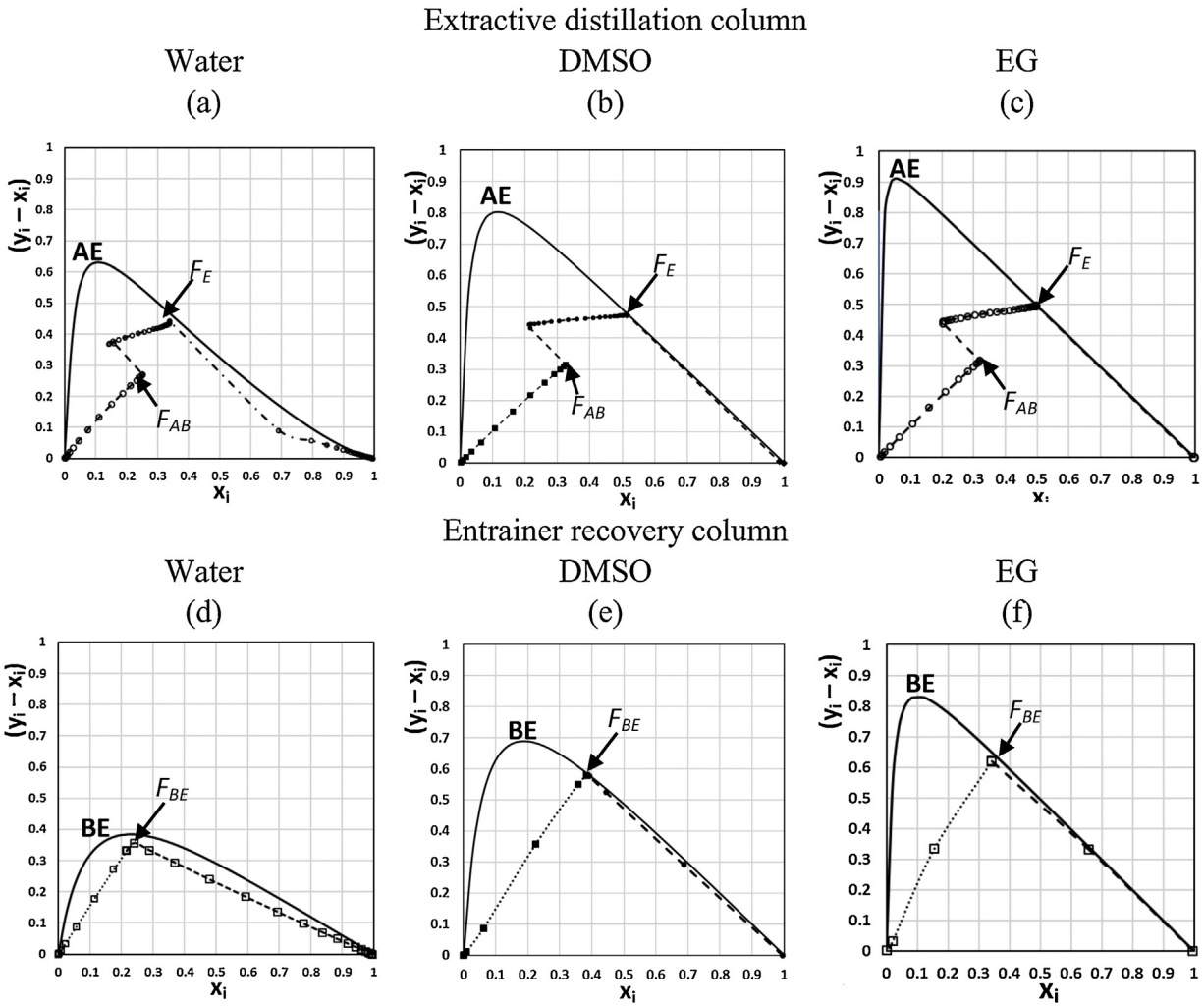

Fig. 7 – Optimal liquid profile into the extractive distillation column and the entrainer recovery column along with driving force diagrams, i: acetone or methanol.

lene glycol achieves the BE separation of methanol–entrainer with less trays and reflux ratio than DMSO and water. According to Bek-Pedersen and Gani (2004), the optimal feed position F_{BE} should be at the maximum value of DF for a binary separation. This is found for water but not for DMSO and ethylene glycol recovery column. We believe this will not be the case in general, because the optimal operation conditions are computed considering both columns together, but more investigation is needed to be more affirmative. Finally, as expected, water having a much lower driving force, it carries out the separation of the methanol–water mixture with much more trays and a greater reflux ratio than the other entrainers.

Fig. 8 shows the optimal liquid profile into the extractive distillation column along with the isovolatility curves in the ternary diagram. Extractive liquid profiles are located in a region of isovolatility values between 2 and 2.5 for the three entrainers. They end up at the entrainer feed tray location near the binary edge AE at $x_E = 0.5$ for both DMSO and EG entrainers and at $x_E = 0.64$ for water. This point is the stable node of the extractive profile map. According to the general feasibility criterion (Rodríguez-Donis et al., 2009a; Shen et al., 2013), it should lie close enough to the edge AE to intersect the rectifying section profile that will reach the distillate product specification. Regarding the x_E value itself, De Figueirêdo et al. (2015) pointed out that the optimized process with minimum TAC is mainly determined by the reflux ratio corresponding to an optimal location of F_E in the ternary diagram at x_E between 0.2 and 0.75, in agreement with our results. Additionally, based on our experience over many case studies, we also observe that the optimal liquid profile of the extractive distillation column is commonly located in the region where $\alpha_{A,B}$ varies between 1.5 and 3 for this diagram class (1.0-1a). In this work, Fig. 8 shows that DMSO and EG extractive profiles are comparable starting at $\alpha_{A,B} = 2$ and reaching the value of $\alpha_{A,B} = 2.75$ at the tray of the azeotrope feeding F_{AB}. For both entrainers, the extractive liquid profile is located in a region where DF_A^{AE} keeps almost stable according to Fig. 7b and c. In the case of water, the extractive profile runs in a region with a smaller increase of $\alpha_{A,B}$ in Fig. 8 that is in agreement with a more significant decrease of the driving force DF_A^{AE} in Fig. 7a.

5. Conclusions

This paper presents preliminary explorations of a framework for computer-aided molecular design of a pure heavy homogeneous entrainer E for separating a minimum boiling azeotrope AB by extractive distillation corresponding to the Serafimov ternary class 1.0-1a. The framework is a systematic approach to convert a Computer-Aided Molecular Design problem for process fluids into a mixed integer non-linear programming (MINLP) problem. The screening of optimal entrainers is based on new thermodynamic criteria involving the maximization of the driving force of the components A and B in their respective mixtures AE and BE under the thermodynamic constraint

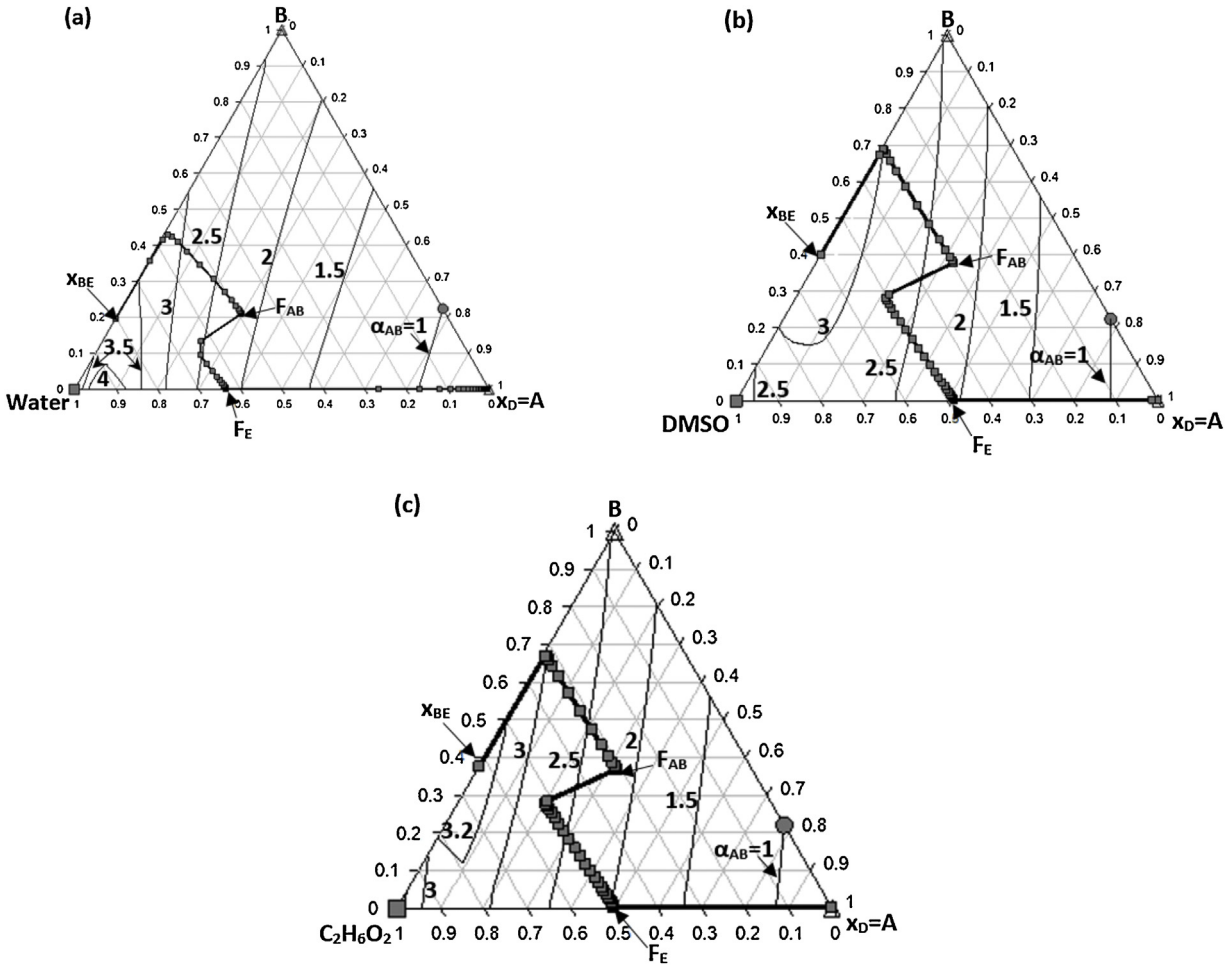

Fig. 8 – Optimal liquid profile into the extractive distillation column and the isovolatility curves maps for water (a), DMSO (b) and ethylene glycol (c).

while constraining the entrainer composition x_E at a given value of the isovolatility curves. Ethylene glycol was obtained as the best entrainer of the initial population. The new criterion with isovolatility constraints shows that EG displays a similar isovolatility curves chart than the best benchmark entrainer DMSO but enhances more the driving force of acetone (A) and methanol (B). Water, another common entrainer, is found much less powerful. Process optimisation confirms the preliminary screening with the water-based process being 30% more costly and energy consuming than DMSO and EG being like DMSO within 4% due to a higher boiling temperature and vaporization enthalpy than DMSO resulting in a greater heat duty $Q_{reboiler}$ in the entrainer recovery column.

The performance of the entrainers is not anticipated properly nor discriminated by literature criteria like $S^{\infty E}_{A,B}$ and $S^{\infty E}_{A,B}C^{\infty E}_{B}$. On the other hand, optimization studies confirm the screening based on the computation of thermodynamic criteria such as driving forces and the entrainer composition at fixed isovolatility value. Design of entrainers selected on this basis allows the separation of the components with low entrainer flow rate, reflux ratio and equilibrium trays number. However, energy related properties as boiling temperature and vaporization enthalpy must also be considered due to their negative effect on the total annual cost. The methodology can be extended to other feasible Serafimov's ternary diagram classes for extractive distillation process such as (1.0-1b), (1.0-2) and (0.0-1) because it is only based on the calculation of thermodynamic parameters.

References

Arlt, W., 2014. Azeotropic distillation. In: Gorak, A., Olujic, Z. (Eds.), Distillation Book, Vol. II Distillation: Equipment and Processes. Elsevier, Amsterdam, pp. 247–259, ISBN 978-0-12-386878-7, Chap. 7.

Babi, D.K., Lutze, P., Woodley, J.M., Gani, R., 2014. A process synthesis intensification framework for the development of sustainable membrane-based operations. Chem. Eng. Process. Process Intensif. 86, 173–195.

Bek-Pedersen, E., Gani, R., 2004. Design and synthesis of distillation systems using a driving-force-based approach. Chem. Eng. Process. 43, 251–262.

Bek-Pedersen, E., Gani, R., Levaux, O., 2000. Determination of optimal energy efficient separation schemes based on driving forces. Comput. Chem. Eng. 24, 253–259.

Brüggemann, S., Marquardt, W., 2004. Shortcut methods for nonideal multicomponent distillation: 3. Extractive distillation columns. AIChE J. 50, 1129–1149.

Bussieck, M., Meeraus, A., 2004. General Algebraic Modeling System (GAMS). Appl. Optim. 88, 137–158.

CEPCI, 2016. CEPCI index for year 2013. Chem. Eng. 123, 92.

Chen, B., Lei, Z., Li, Q., Li, C., 2005. Application of CAMD in separating hydrocarbons by extractive distillation. AIChE J. 51, 3114–3121.

Cignitti, S., Zhang, L., Gani, R., 2015. Computer-aided framework for design of pure, mixed and blended products. Comput. Aided Chem. Eng. 37, 2093–2098.

Conte, E., Gani, R., Ng, K.M., 2011. Design of formulated products: a systematic methodology. AIChE J. 57, 2431–2449.

Constantinou, L., Gani, R., 1994. New Group Contribution Method for Estimating Properties of Pure Compounds. AIChE J. 40, 1697–1710.
Constantinou, L., Gani, R., O'Connell, J., 1995. Estimation of the acentric factor and the liquid molar volume at 298 K using a new group contribution method. Fluid Phase Equilibr. 103, 11–22.
De Figueirêdo, M.F., Guedes, B.P., de Araújo, J.M.M., Vasconcelos, L.G.S., Brito, R.P., 2011. Optimal design of extractive distillation columns—a systematic procedure using a process simulator. Chem. Eng. Res. Des. 89, 341–346.
De Figueirêdo, M.F., Brito, K.D., Ramos, W.B., Vasconcelos, L.G.S., Brito, R.P., 2015. Effect of solvent content on the separation and the energy consumption of extractive distillation columns. Chem. Eng. Commun. 202, 1191–1199.
Douglas, J.M., 1988. Conceptual Design of Chemical Processes. McGraw-Hill, New York.
Fredenslund, A., Jones, R.L.R., Prausnitz, J.M.J., 1975. Group-contribution estimation of activity coefficients in nonideal liquid mixtures. AIChE J. 21, 1086–1099.
Frits, E.R., Lelkes, Z., Fonyó, Z., Rév, E., Markót, M.C., Csendes, T., 2006. Finding limiting flows of batch extractive distillation with interval arithmetic. AIChE J. 52, 3100–3108.
Gani, R., Bek-Pedersen, E., 2000. Simple new algorithm for distillation column design. AIChE J. 46, 1271–1274.
Gerbaud, V., Rodriguez-Donis, I., 2014. Extractive distillation. In: Gorak, A., Olujic, Z. (Eds.), Distillation Book, Vol. II Distillation: Equipment and Processes. Elsevier, Amsterdam, pp. 201–246, ISBN 978-0-12-386878-7, Chap. 6.
Gerbaud, V., Rodriguez-Donis, I., Lang, P., Denes, F., Hegely, L., You, X., 2019. Review of extractive distillation: process design, operation optimization and control. Chem. Eng. Res. Des. 141, 229–271.
Hukkerikar, A.S., Sarup, B., Ten Kate, A., Abildskov, J., Sin, G., Gani, R., 2012. Group-contribution + (GC +) based estimation of properties of pure components: improved property estimation and uncertainty analysis. Fluid Phase Equilib. 321, 25–43.
Kiva, V.N., Hilmen, E.K., Skogestad, S., 2003. Azeotropic phase equilibrium diagrams: a survey. Chem. Eng. Sci. 58, 1903–1953.
Knapp, J.P., Doherty, M.F., 1994. Minimum entrainer flows for extractive distillation: a bifurcation theoretic approach. AIChE J. 40, 243–268.
Kossack, S., Kraemer, K., Gani, R., Marquardt, W., 2008. A systematic synthesis framework for extractive distillation processes. Chem. Eng. Res. Des. 86, 781–792.
Laroche, L., Bekiaris, N., Andersen, H.W., Morari, M., 1991. Homogeneous azeotropic distillation: comparing entrainers. Can. J. Chem. Eng. 69, 1302–1319.
Laroche, L., Bekiaris, N., Andersen, H.W., Morari, M., 1992a. Homogeneous azeotropic distillation: separation and flowsheet synthesis. Ind. Eng. Chem. Res. 31, 2190–2209.
Laroche, L., Bekiaris, N., Andersen, H.W., Morari, M., 1992b. The curious behavior of homogeneous azeotropic distillation — implications for entrainer selection. AIChE J. 38, 1309–1328.
Lei, Z., Li, C., Chen, B., 2003. Extractive distillation: a review. Sep. Purif. Rev. 32 (2), 121–213.
Lelkes, Z., Lang, P., Benadda, B., Moszkowicz, P., 1998. Feasibility of extractive distillation in a batch rectifier. AIChE J. 44 (4), 810–822.
Levy, S.G., Van Dongen, D.B., Doherty, M.F., 1985. Design and synthesis of homogeneous azeotropic distillations. 2. Minimum reflux calculations for nonideal and azeotropic columns. Ind. Eng. Chem. Fundamen. 24 (4), 463–474.
Luyben, W.L., Chien, I.L., 2010. Design and Control of Distillation Systems for Separatin Azeotropes. Wiley-VCH, New York, pp. 453.
Momoh, S.O., 1991. Assessing the accuracy of selectivity as a basis for solvent screening in extractive distillation processes. Sep. Sci. Technol. 26 (5), 729–742.
Odele, O., Macchietto, S., 1993. Computer aided molecular design: a novel method for optimal solvent selection. Fluid Phase Equilib. 82, 47–54.
Petlyuk, F.B., Danilov, R.Yu., 1999. Sharp distillation of azeotropic mixtures in a two-feed column. Theor. Found. Chem. Eng. 33, 233–242.
Petlyuk, F., Danilov, R., Burger, J., 2015. A novel method for the search and identification of feasible splits pf extractive distillations in ternary mixtures. Chem. Eng. Res. Des. 99, 132–148.
Pretel, E.J., López, P.A., Bottini, S.B., Brignole, E.A., 1994. Computer-aided molecular design of solvents for separation processes. AIChE J. 40 (8), 1349–1360.
Rodríguez-Donis, I., Gerbaud, V., Joulia, X., 2009a. Thermodynamic insights on the feasibility of homogeneous batch extractive distillation. 1. Azeotropic mixtures with heavy entrainer. Ind. Chem. Eng. Res. 48 (7), 3544–3559.
Rodríguez-Donis, I., Gerbaud, V., Joulia, X., 2009b. Thermodynamic insights on the feasibility of homogeneous batch extractive distillation, 2. Low-relative-volatility binary mixtures with a heavy entrainer. Ind. Chem. Eng. Res. 48 (7), 3560–3572.
Rodríguez-Donis, I., Gerbaud, V., Joulia, X., 2012a. Thermodynamic insights on the feasibility of homogeneous batch extractive distillation. 3. Azeotropic mixtures with light boiling entrainer. Ind. Chem. Eng. Res 51, 4643–4660.
Rodríguez-Donis, I., Gerbaud, V., Joulia, X., 2012b. Thermodynamic insights on the feasibility of homogeneous batch extractive distillation, 4. Azeotropic mixtures with intermediate boiling entrainer. Ind. Chem. Eng. Res. 51, 6489–6501.
Sánchez-Daza, O., Pérez-Cisneros, E.S., Bek-Pedersen, E., Gani, R., 2003. Graphical and stage-to-stage methods for reactive distillation column design. AIChE J. 49, 2822–2841.
Shen, W., Gerbaud, V., 2013. Extension of thermodynamic insights on batch extractive distillation to continuous operation. 2. Azeotropic mixtures with a light entrainer. Ind. Eng. Chem. Res. 52 (12), 4623–4637.
Shen, W., Benyounes, H., Gerbaud, V., 2013. Extension of thermodynamic insights on batch extractive distillation to continuous operation. 1. Azeotropic mixtures with a heavy entrainer. Ind. Eng. Chem. Res. 52 (12), 4606–4622.
Shen, W., Dong, L., Wei, S., Li, J., Benyounes, H., You, X., Gerbaud, V., 2015. Systematic design of an extractive distillation for maximum-boiling azeotropes with heavy entrainers. AIChE J. 61 (11), 3898–3910.
Skiborowski, M., Rautenberg, M., Marquardt, W., 2015. An hybrid evolutionary — deterministic optimization approach for conceptual design. Ind. Eng. Chem. Res. 54, 10054–10072.
Tula, A.K., Eden, M.R., Gani, R., 2015. Process synthesis, design and analysis using a process-group contribution method. Comput. Chem. Eng. 81, 245–259.
Wahnschafft, O.M., Westerberg, A.W., 1993. The product composition regions of azeotropic distillation columns: 2. Separability in two-feed columns and entrainer selection. Ind. Eng. Chem. Res. 32, 1108–1120.
You, X., Rodriguez-Donis, I., Gerbaud, V., 2014. Extractive distillation process optimisation of the 1.0-1a class system, acetone–methanol with water. Comput. Aided Chem. Eng. 33, 1315–1320.
You, X., Rodriguez-Donis, I., Gerbaud, V., 2015a. Improved design and efficiency of the extractive distillation process for acetone-methanol with water. Ind. Eng. Chem. Res. 54 (1), 491–501.
You, X., Rodriguez-Donis, I., Gerbaud, V., 2015b. Investigation of separation efficiency Indicator for the optimization of the acetone-methanol extractive distillation with water. Ind. Eng. Chem. Res. 54 (43), 10863–10875.
You, X., Rodriguez-Donis, I., Gerbaud, V., 2016. Low pressure design for reducing energy cost of extractive distillation for separating diisopropyl ether and isopropyl alcohol. Chem. Eng. Res. Des. 109, 540–552.